

Numerical study of the accuracy and reproducibility of sound absorption measurements in reverberation rooms at low frequencies

Paul Didier^{a,*}, Cédric Van hoorickx^a, Edwin P.B. Reynders^a

^a*KU Leuven, Department of Civil Engineering, Structural Mechanics Section
Kasteelpark Arenberg 40, B-3001 Leuven, Belgium*

Abstract

Standardised absorption measurements in reverberation rooms suffer from relatively low reproducibility, especially at low frequencies and for highly absorptive samples. In these conditions, complete sound field diffusivity cannot be achieved. However, recent research has demonstrated that the theoretical diffuse absorption emerges as the ensemble average across a wide range of rooms with different geometries, even at very low frequencies. The present study aims to investigate the influence of the room geometry, sound source positioning, and presence of panel diffusers on the sound absorption values obtained in a specific reverberation room, as well as on the difference between those values and the theoretical diffuse values. The focus is on the lowest frequency bands.

A numerical simulation approach is proposed, in which the room without sample is modeled in full detail using the finite element method and coupled to the sample with a Rayleigh-Ritz approach. The measurement of diffuse sound absorption is simulated in an efficient way using a stationary power balance approach. This approach is validated against measured data and against a detailed simulation of the impulse response. From the parametric study conducted with the model, it can be concluded that, for highly absorptive samples, good agreement with the theoretical diffuse absorption values can be obtained for certain room designs. In these rooms, the measured absorption is also less sensitive to the number and positioning of sources and diffusing elements.

Keywords: room acoustics, sound absorption, reverberation room method, reproducibility

1. Introduction

Significant variations in the outcome of sound absorption measurements using the reverberation room method have been experimentally witnessed for decades [1–3]. Measurements of the same absorptive material conducted in different reverberation rooms may yield non-negligibly disparate results, even though all involved laboratories follow the same standardised procedure. This variability is particularly noticeable below 300 Hz, as underlined in a recent round robin study [4] conducted across many existing reverberation rooms, where the authors systematically followed a recently proposed revised version of the ISO 354:2003 standard for sound absorption measurements [5], ISO/CD 354:2019 [6]. The magnitude of the produced uncertainties showed that, still today, the measurement of sound absorption suffers from insufficient reproducibility especially at low frequencies.

One of the factors known to significantly contribute to the variability of low-frequency sound absorption measurements is the lack of sound field diffusivity in that range [4, 7, 8]. Indeed, the reverberation room sound absorption measurement method relies on the assumption of sufficient sound field diffusivity [5], as absorption coefficients are obtained from reverberation times through Sabine’s formula [9], which assumes

*Corresponding author

Email address: paul.didier@kuleuven.be (Paul Didier)

Postprint submitted to Applied Acoustics

Published version: P. Didier, C. Van hoorickx, and E.P.B. Reynders. Numerical study of the accuracy and reproducibility of sound absorption measurements in reverberation rooms at low frequencies. *Applied Acoustics*, 200:109047, 2022. <https://doi.org/10.1016/j.apacoust.2022.109047>

15 a uniform sound pressure level over the entire room. Following the definition given by the random wave theory, a diffuse sound field is a superposition of many plane waves with uncorrelated phases and amplitudes and uniformly distributed directions of incidence [10]. This idealised concept cannot be exactly reproduced in reality, yet may serve as an adequate approximation in a rigid enclosure at high frequencies [10]. At low frequencies, however, the sound field exhibits a low modal overlap and therefore strongly depends on the
20 particular modal behaviour of the reverberation room. In that frequency range, distinct room resonances appear at specific combinations of positions and frequencies and render the sound field non-diffuse. The modal behaviour of the reverberation room is itself dictated by the room geometry and the presence of additional diffusing elements. Furthermore, the location of sound sources determines the degree to which each room mode is excited [11]. Other factors known to have the potential to impact sound absorption
25 measurements reproducibility at low frequencies are the sample size effect [12] and the position of the absorptive material [13]. These latter two aspects are, however, not investigated in the present work – the sample placement and the sample size are kept fixed in all simulations.

To evaluate the performance of a given reverberation room geometry, benchmark sound absorption coefficient values must be set. They represent the values that would be consistently obtained in a perfectly
30 diffuse field under ideal measurement conditions. It has been recently demonstrated that, although the low-frequency sound field in a single reverberation room cannot be considered diffuse, the theoretical diffuse sound absorption coefficients equals the ensemble average over a wide set of (reverberation) rooms [14]. The conceptual rooms comprised in this set have the same total absorption area and modal density but otherwise consist of any random arrangement of boundaries and/or scattering elements. It has also been
35 demonstrated in [14] that the theoretical diffuse absorption value of a finite-sized sample, which is modeled in full detail (e.g., using the finite element method) including boundary conditions, can be rigorously obtained by application of the diffuse field reciprocity relationship [15]. This relationship also underpins a general method of analysis of built-up systems consisting of deterministic and diffuse components [16, 17] as well as dedicated methods for quantifying airborne [18, 19] and impact [20, 21] sound insulation prediction.

40 The low-frequency sound field inside geometrically regular cavities such as cylinders or cuboids can be well described via closed-form analytical expressions, often expressing the sound pressure as a sum where each term depends on a mode of the cavity [11, 22]. However, in the more general case where the geometry is not bounded to simple shapes, low-frequency sound field modelling requires the use of more complex numerical methods. At low frequencies, wave-based approaches are popular in the literature since
45 geometrical acoustics-based methods rely on the assumption that sound waves act as rays and propagate in straight lines through the air, which is only valid at high frequencies [23]. General numerical methods such as finite element (FE), boundary element, or finite difference methods have been widely used to solve the wave or Helmholtz equation for complex geometries and boundary conditions at low frequencies. Attempts were recently made to bridge the gap between low frequencies and geometrical acoustics [24], yet strong
50 evidence of their validity remains scarce. Many authors have investigated the high-frequency sound field in reverberation rooms via geometrical acoustics-based methods [7, 25–27] and wave-based modelling has been employed by others to investigate the low-frequency behaviour of reverberation rooms [28–32]. One important drawback of the methods that heavily rely on FE computations is their large computational cost [23]. In this work, this issue is mitigated by combining FE modelling with an analytical method. A
55 FE model of the reverberation room is constructed, allowing the numerical representation of any room shape. The room’s undamped eigenfrequencies and mode shapes are computed via modal analysis. These quantities are then used as inputs to the analytical Lagrange-Rayleigh-Ritz (or assumed-modes) method [33], where the pressure field is expanded onto the basis formed by the hard-walled room mode shapes. The presence of an absorptive sample is taken into account in the pressure field formulation through a localised
60 boundary condition, independently of the basis functions chosen for the pressure expansion. This technique is computationally much cheaper than a direct harmonic analysis. Similar approaches, sometimes referred to as modal decompositions, have been used by some of the aforementioned studies on the low-frequency sound field in reverberation rooms [30, 32]. In the present work, the total energy and input power in the room with or without the presence of the absorptive sample are derived directly from the generalised coordinates of the pressure expansion. The absorption coefficient can then be estimated from a power balance [34]. This
65 methodology produces a good agreement with results obtained using the standardised integrated impulse

response (IIR) method [5]. While the power balance method considers the sound field in its entirety, the IIR method relies on the explicit computation of frequency response functions and is, therefore, inherently prone to uncertainties generated by the choice of microphone positions, especially at low frequencies [27]. In this work, the effect of precise microphone positioning on sound absorption measurements is disregarded since the associated uncertainties can theoretically be arbitrarily reduced by increasing the number of measurement positions. The complete absorption coefficient retrieval method used in this study is validated against real measurement data.

The aforementioned framework allows the efficient simulation of various low-frequency sound absorption measurement scenarios where, among other parameters, the shape of the reverberation room, the source position, and the size and placement of the sample may be arbitrarily defined. Diffusing elements such as hanging panels may also be introduced as part of the FE model. The effect of sound source number and positioning, number of panel diffusers, and room shape on low-frequency sound absorption measurements are investigated in this paper. Similar parametric studies have been conducted in the past, although mainly via experimental approaches based on the standardised IIR method [5, 7, 8, 27, 35]. Experimental parametric studies are costly and time-consuming, and therefore usually limited in the number of independently varied parameters. The method presented here allows to complement such studies with many additional simulations of high accuracy, and this at a much lower computation cost than via direct FE simulation of the experimental test procedure.

This paper is organised as follows. The methodology is outlined in Section 2, presenting the power balance method used to simulate sound absorption measurement, a comparison of the latter to measured data, the precise models used for the reverberation room and the absorber, and the hybrid deterministic-statistical energy analysis (det-SEA) method via which the theoretical diffuse absorption coefficients are derived. Section 3 compares and discusses the outcomes of simulated measurements conducted in six different reverberation room designs with different sound sources layouts. A simulated evaluation of the impact of panel diffusers on low-frequency sound absorption measurements is presented and discussed in Section 4. Conclusions and potential future research directions are finally provided in Section 5.

2. Methodology

2.1. Numerical estimation of absorption coefficients

To study the outcomes of sound absorption measurements using a numerical approach, one must be able to simulate such measurement in all relevant environments. In the context of this study, this implies any reverberation room design, with any combination of sources, in the presence of a finite absorptive sample, and potentially including panel diffusers.

This problem can be intuitively tackled by replicating one of the standardised experimental methods described in the ISO 354:2003 [5] and ISO/CD 354:2019 [6]: (i) the interrupted noise method or (ii) the IIR method. Both methods consist in determining the reverberation time from the slope of energy decays for several combinations of source and receiver locations. Following method (i), the decaying sound pressure is directly recorded after interruption of a wide-band noise source, or, following method (ii), room impulse responses are determined and backwards-integrated following Schroeder's methodology [10] to obtain energy decay curves. The final absorption coefficient is then defined via Sabine's equation [9] from the average over the reverberation time estimates obtained at each combination of source and microphone location. The IIR methodology, used in this paper for validating the proposed approach, may be replicated by first extracting frequency response functions (FRFs) through analysis of the simulated sound field at specific locations in the FE model of the reverberation room, with and without the sample. The room impulse responses can then be obtained via the inverse Fourier transforms of those FRFs. However, reverberation time estimates can be highly sensitive to the number and precise positions of microphone measurement points [27].

This discrete spatial sampling is one of the factors contributing to a sometimes poor repeatability in actual measurement scenarios – although the acoustic scenario remained unchanged, sequential sound absorption measurements may yield different results simply due to a change in microphone layout. Directly replicating these measurement methods is therefore not ideal when attempting to isolate the respective effects of,

e.g., room shape or presence of panel diffusers, as it is inherently subject to uncertainties related to the microphone layout. In theory, one may arbitrarily reduce the uncertainty due to the discrete spatial sampling of the sound field by increasing the number of microphone positions, tending towards a perfect sampling where all possible microphone positions are considered.

120 An alternative method to retrieve absorption coefficients considers the sound field inside reverberation rooms from an energetic standpoint, thereby removing the need for discrete measurement locations. It is referred to hereafter as the *power balance method*. The absorption coefficient may indeed be expressed via energetic quantities by first considering the power balance for a stationary harmonic excitation at angular frequency ω :

$$P_{\text{in}} = \omega\eta E = \frac{6 \ln(10)}{T} E, \quad (1)$$

125 where P_{in} denotes the input power, E the total energy in the reverberation room, η the total damping loss factor, and T the reverberation time. Eq.(1) holds both in the empty reverberation room and in the reverberation room with an absorptive sample. A harmonic expression of the absorption coefficient $\alpha(\omega)$ in terms of energetic quantities can be obtained by isolating the reverberation time T in Eq.(1) and substituting it into Sabine's formula [9]:

$$\alpha_{\text{sim}}(\omega) = \frac{24 \ln(10)}{c_0 S_A} \left(\frac{V_s}{T_s} - \frac{V_e}{T_e} \right) = \frac{4}{c_0 S_A} (V_s \omega \eta_s - V_e \omega \eta_e) = \frac{4}{c_0 S_A} \left(\frac{P_{\text{in},s}}{E_s} V_s - \frac{P_{\text{in},e}}{E_e} V_e \right), \quad (2)$$

130 where the indices "e" and "s" refer to the empty reverberation room case and the reverberation room with sample case, respectively, c_0 is the speed of sound in air, S_A is the absorptive sample surface area exposed to the sound field, and V is the volume of air in the reverberation room. The subscript "sim" is used to remove any notation ambiguity between this absorption coefficient, estimated for a particular reverberation room geometry, and the theoretical diffuse value obtained via the method that will be described in Section 2.5.
 135 A noteworthy advantage of the power balance method is that it enables the derivation of the harmonic absorption coefficient $\alpha_{\text{sim}}(\omega)$. To compute the standardised 1/3-octave band coefficients from the output of Eq.(2), an integration over frequency suffices:

$$\alpha_{\text{sim}}(\omega_c) = \frac{1}{\omega_h - \omega_l} \int_{\omega_l}^{\omega_h} \alpha_{\text{sim}}(\omega) d\omega, \quad (3)$$

where $\omega_h = 2\pi f_h$ and $\omega_l = 2\pi f_l$ respectively denote the high- and low-band edge angular frequencies of the 1/3-octave band centred on $\omega_c = 2\pi f_c = 2\pi f_h \cdot 2^{-1/6} = 2\pi f_l \cdot 2^{1/6}$.

140 As Eq.(2) shows, one may derive E and P_{in} in order to estimate the harmonic absorption coefficient. The next paragraphs describe the sequence of steps used to compute these energetic quantities. First, the sound pressure $p(\mathbf{r}, \omega)$ at a point \mathbf{r} and an angular frequency ω in the reverberation room may be expressed analytically following a Rayleigh-Ritz approach [34]. In the presence of a finite absorptive sample, the acoustic system may be described as a damped cavity for which the interior problem is of interest.
 145 The sound pressure field at a point \mathbf{r} inside the reverberation room existing in the presence of a localised point source at \mathbf{r}_0 can be described via the inhomogeneous Helmholtz equation combined with admittance boundary conditions accounting for damping in the cavity. Some assumptions are made at this stage: (i) the finite absorptive sample is locally reacting with a constant normalised surface admittance β (which can be calculated using an analytical model or a transfer matrix method [34]) over its surface, (ii) the other surfaces
 150 of the reverberation room are rigid, and (iii) there is a weak mechanical coupling between the absorptive sample and the sound field. Note that no assumption is made on the nature of the absorptive sample's surface; non-planar absorbers can be considered using this method. Considering the integral formulation for the interior problem, as derived in detail in [34] from the inhomogeneous Helmholtz equation and additional boundary conditions, these assumptions allow a reduction of the span of the first integral term down to the
 155 surface of the absorptive sample:

$$p(\mathbf{r}, \omega) \approx -jk\beta \int_{\partial\Omega_A} G(\mathbf{r}, \mathbf{y}, \omega) p(\mathbf{y}, \omega) d\mathbf{y} + j\omega\rho_0 Q_s G(\mathbf{r}, \mathbf{r}_0, \omega), \quad (4)$$

$$G(\mathbf{r}_1, \mathbf{r}_2, \omega) = \sum_{i=1}^N \frac{\phi_i(\mathbf{r}_1)\phi_i(\mathbf{r}_2)}{\omega_i^2(1 + j\eta_r(\omega)) - \omega^2}, \quad (5)$$

where k is the wavenumber, $\partial\Omega_A$ is the surface of the absorptive sample exposed to the sound field in the reverberation room (of area S_A), ρ_0 is the density of air, Q_s is the volume velocity of the source, and ϕ_i and ω_i are the mode shape and eigenfrequency of the i^{th} hard-walled reverberation room mode, respectively. In the denominator of the Green's function $G(\mathbf{r}_1, \mathbf{r}_2, \omega)$ in Eq.(5), $\eta_r(\omega)$ represents the frequency-dependent inherent damping loss factor of the reverberation room (without absorber present), which accounts for all possible sources of damping in the empty room. Note that, in practice, only a finite number N of modes can be considered in the computation of $G(\mathbf{r}_1, \mathbf{r}_2, \omega)$. In this study, N is systematically chosen such that the largest angular eigenfrequency $\omega_{i=N}$ is equal to 1.5ω , where ω is the angular frequency of analysis. This ensures that all room modes able to noticeably influence the sound field at the frequency of analysis are included in the computation.

In parallel to Eq.(4), the Lagrange-Rayleigh-Ritz or assumed-modes approach [34] is considered, where $p(\mathbf{r}, \omega)$ is expanded onto an orthogonal basis. Here, the chosen basis is formed by the hard-walled room mode shapes, following the assumption of rigid walls outside of the absorptive sample area. This yields:

$$p(\mathbf{r}, \omega) = \sum_{i=1}^N \phi_i(\mathbf{r})q_i(\omega). \quad (6)$$

Substituting Eq.(6) into Eq.(4) and rearranging terms provides an expression for the generalised coordinates of the expansion as a function of the angular frequency ω , $\mathbf{q}(\omega) = [q_1(\omega) \dots q_N(\omega)]^T$. In the empty reverberation room and in the reverberation room with a sample present ($\mathbf{q}_e(\omega)$ and $\mathbf{q}_s(\omega)$, respectively), this may be expressed in matrix form as:

$$\mathbf{q}_e(\omega) = (\mathbf{\Omega}^2(1 + j\eta_r(\omega)) - \omega^2\mathbf{I})^{-1} \mathbf{f}(\omega) \quad \text{and} \quad \mathbf{q}_s(\omega) = (\mathbf{\Omega}^2(1 + j\eta_r(\omega)) - \omega^2\mathbf{I} + jk\rho_0c_0\beta\mathbf{C})^{-1} \mathbf{f}(\omega), \quad (7)$$

where $\mathbf{\Omega}$ denotes the diagonal matrix containing the N lowest hard-walled eigenfrequencies of the reverberation room ($[\mathbf{\Omega}]_{i,j} = \omega_i \forall i = j, 0$ otherwise), \mathbf{C} the $N \times N$ coupling matrix containing all cross-products of hard-walled modes shapes integrated over the exposed absorber surface $\partial\Omega_A$ (i.e., $[\mathbf{C}]_{i,j} = \int_{\partial\Omega_A} \phi_i(\mathbf{r})\phi_j(\mathbf{r})d\mathbf{r}$), $\mathbf{f}(\omega)$ the modal force term representing the exciting sources in the room, and c_0 the speed of sound. Note that $\mathbf{q}_e(\omega)$ is simply obtained from $\mathbf{q}_s(\omega)$ by setting β to null (no added absorption in the empty reverberation room). In practice, the terms in \mathbf{C} are computed using a two-dimensional numerical integration over a flat grid of points covering the absorptive sample's surface exposed to the sound field.

Although Eq.(4) is an approximation of the true pressure field due to the assumptions made, its outcome agrees well with direct harmonic analysis of the FE model while substantially reducing the computational effort. An example of this good agreement is shown in Fig.1 where FRFs derived, on one hand, via a modal analysis of the FE model followed by a derivation of the generalized coordinates in Eq.(7) then utilised in Eq.(6) and, on the other hand, via a direct harmonic analysis of the FE model are compared. The harmonic and modal analyses are computed at specific points in the FE model to be able to extract the FRFs using both methods. Note that, in the remainder of this paper, the empty-room volume is fixed in order to avoid any influence that the room volume could have on the comparison between rooms with different geometries. All room geometries are scaled to obtain an empty room volume $V_e = 250 \text{ m}^3$. This value lies within the preferred range mentioned in the ISO/CD 354:2019 [6]. In the particular example shown in Fig.1, the FRFs derived via Eq.(6) require 50 times less computation time than those derived via harmonic analysis. The small observable discrepancies, originating from the Lagrange-Rayleigh-Ritz approximation, have a similar magnitude to those reported in [30], where FRFs obtained via direct harmonic analysis of an FE model were also compared with those obtained with a method based on a modal superposition analogous to Eq.(6). Nevertheless, these small differences do not significantly impact the absorption coefficients that can be obtained from these FRFs using the integrated impulse response method [5]. As will be seen later on, the values obtained using that method agree with measured data.

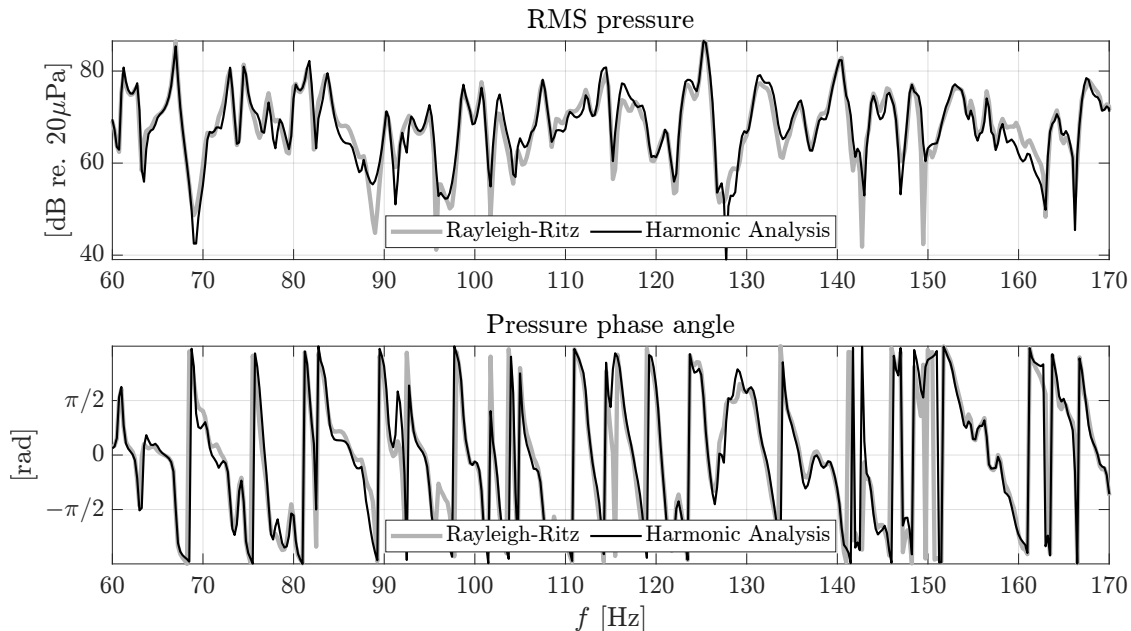


Figure 1: FRF (top: magnitude; bottom: phase) at $\mathbf{r} = (6.63 \text{ m}, 3.79 \text{ m}, 3.03 \text{ m})$ in the KU Leuven reverberation room scaled up to 250 m^3 and excited at $\mathbf{r}_0 = (0.49 \text{ m}, 0.57 \text{ m}, 0.51 \text{ m})$ by a unit volume velocity point source. The $3 \times 3.6 \times 0.2 \text{ m}^3$ porous absorber present in the room is modelled as a Delany-Bazley-Miki [36, 37] equivalent fluid of flow resistivity $\sigma = 10.9 \text{ kN} \cdot \text{s} \cdot \text{m}^{-4}$. The FRF is either retrieved via a fine-resolution direct harmonic analysis (black) or via a modal analysis combined with the Rayleigh-Ritz approach [Eq.(4)] (grey).

The generalised coordinates obtained via Eq.(7) are independent of the precise location \mathbf{r} and can be used to express the total energy and the input power in the reverberation room, as:

$$E = \frac{1}{4\rho_0\omega^2} \sum_{i=1}^N (\omega^2 + \omega_i^2) |q_i(\omega)|^2 \quad \text{and} \quad P_{\text{in}} = -\frac{1}{2\rho_0\omega} \text{Im} \left\{ \sum_{i=1}^N f_i^*(\omega) q_i(\omega) \right\}, \quad (8)$$

where $*$ represents the complex conjugate operator and $f_i(\omega)$ the i^{th} element of the modal force vector. Inserting the outcomes of Eq.(8) into Eq.(2) eventually yields a harmonic estimate of the measured absorption coefficient in the particular reverberation room considered. Note that the pressure $p(\mathbf{r}, \omega)$, although possible to compute in the empty room (respectively, in the room with an absorptive sample) by substituting the generalised coordinates \mathbf{q}_e (respectively, \mathbf{q}_s) and mode shapes $\{\phi_i\}_{i=1}^N$ in Eq.(6), does not need to be computed to obtain α_{sim} using this method.

Since the ISO 354:2003 standard imposes the use of at least two source positions in practice [5], one must be able to model the presence of multiple sound sources. Although it is possible to simply perform sequential simulations with a single, different source position each time, there exists a more efficient alternative. By decorrelating the signals fed to each individual sound source, an arbitrary number of sources N_s may simultaneously excite the room without interfering with each other. This way, the analysis is performed in a single simulation run instead of N_s runs. The individual source positions are hereafter denoted $\{\mathbf{r}_{0,j}\}_{j=1}^{N_s}$. The decorrelation is performed using phase factors $\{\Psi_j(\omega)\}_{j=1}^{N_s} = \{\exp(j\varphi_j(\omega))\}_{j=1}^{N_s}$ where $\{\varphi_j(\omega)\}_{j=1}^{N_s}$ are real numbers drawn from a continuous uniform distribution between 0 and 2π . A different random phase factor is applied at each frequency ω , mutually decorrelating the individual frequency components generated by each source. The j^{th} phase factor $\Psi_j(\omega)$ is multiplied to every mode shape $\{\phi_i\}_{i=1}^N$ at the j^{th} individual source location $\mathbf{r}_{0,j}$. The presence of sound sources is represented in the modal force term in Eq.(7) and (8). In a multiple sources scenario, the elements of this vector $\mathbf{f}(\omega) = [f_1(\omega) \dots f_N(\omega)]^T$ are computed as:

$$f_i(\omega) = j\rho_0\omega Q_s \sum_{j=1}^{N_s} \Psi_j(\omega)\phi_i(\mathbf{r}_{0,j}). \quad (9)$$

In short, sound absorption measurements can be simulated without relying on a discrete sound field sampling or frequency band processing by (i) conducting a modal analysis of the undamped reverberation room FE model to extract its hard-walled eigenfrequencies and modes shapes, (ii) using these values to derive the generalised coordinates of the expanded sound pressure in the reverberation room with or without an absorptive sample present, and (iii) computing the total energy and input power in the reverberation room from those generalised coordinates in both scenarios, accounting for the potential presence of multiple uncorrelated sound sources. The complete simulation process is summarised as a block diagram in Fig.2.

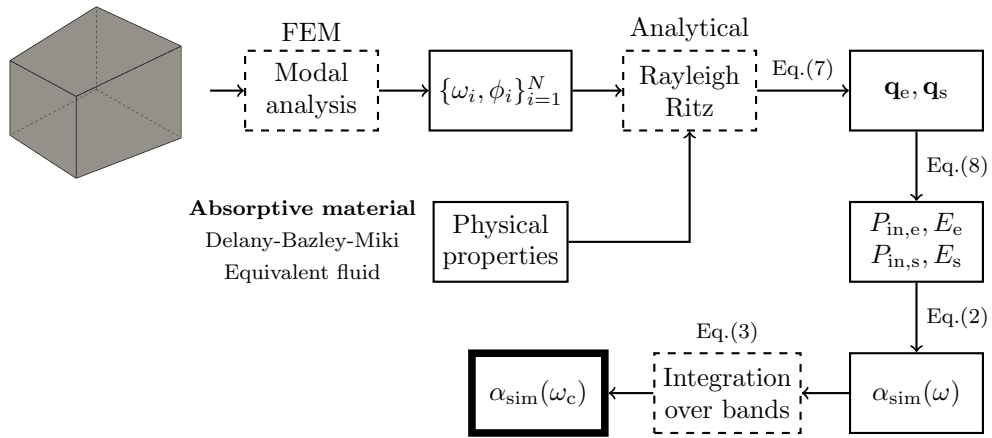


Figure 2: Block-diagram of the processing steps used in this work to simulate sound absorption measurements in a particular reverberation room geometry, given the physical properties of a finite sample of absorptive material.

The equivalence between results yielded by the power balance method and the IIR method is verified in various simulated measurement scenarios. An example is provided in Fig.3, where the reverberation times in 1/3-octave bands estimated using the power balance method are compared to those estimated using the IIR method in a $6 \times 7 \times 5$ m³ perfect cuboid. The empty-room absorption coefficients are arbitrarily set to $\{0.0451, 0.0638, 0.0752, 0.1053, 0.1975\}$ for the 1/3-octave bands centred on $f_c = \{100, 125, 160, 200, 250\}$ Hz, respectively. A single point source is placed close to a corner of the reverberation room and 12 receivers are scattered around the available space – the specific coordinates used in this example are listed in Table 1. Good agreement is found in all bands considered. In addition to confirming the correspondence between the two methods, the results presented in Fig.3 also illustrate the potentially problematic variability of single reverberation time estimates obtained via the IIR method using different microphone positions scattered across the room.

	S	M1	M2	M3	M4	M5	M6	M7	M8	M9	M10	M11	M12
x [m]	0.5	4.95	5.3	3.24	1.19	1.25	1.79	4.7	1.77	4.57	1.72	5.15	2.25
y [m]	0.6	5.85	6.26	3.78	1.33	1.4	2.05	5.54	2.03	5.39	1.96	6.08	2.6
z [m]	0.55	4.06	4.34	2.69	1.05	1.1	1.53	3.86	1.52	3.76	1.47	4.22	1.9

Table 1: Coordinates of source (S) and microphone (M) positions in cuboidal room used for example of correspondence between power balance and IIR method outcomes.

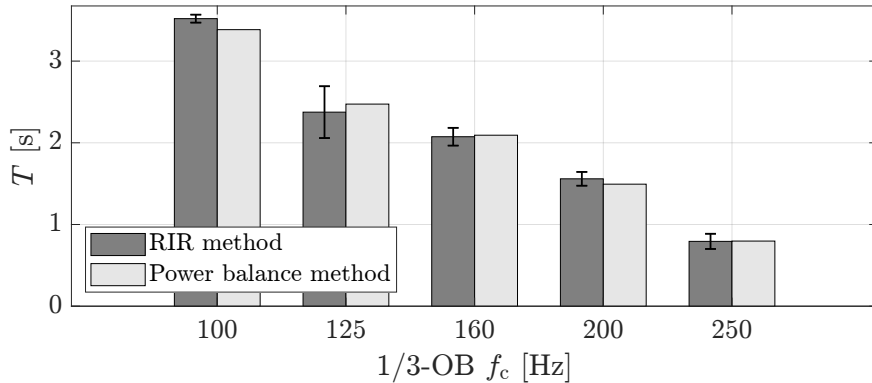


Figure 3: Simulated reverberation times per 1/3 octave band in a $6 \times 7 \times 5 \text{ m}^3$ reverberation room obtained using either the IIR method (dark grey bars, average over 12 random receiver positions scattered across the reverberation room) or the power balance method (light grey bars). The error bars show the standard deviation of results obtained across the 12 individual estimates. Source and microphone coordinates are given in Table 1.

2.2. Reverberation room model

For arbitrarily shaped reverberation rooms, the volume of air contained in the room can be discretised using the finite element method for evaluating the Helmholtz equation at virtually any point and any frequency. This can be achieved in the time domain (transient analysis) or the frequency domain (harmonic or modal analysis). The focus of this study is directed onto the frequency domain, allowing efficient simulations of sound absorption measurements using the power balance method described in Section 2.1. All FE modelling is conducted using the engineering simulation software Ansys and the Ansys Parametric Design Language (APDL) [38]. Second-order tetrahedral finite elements are used. The edge length e of every element in the model is upper bounded by a fourth of the smallest wavelength involved in the computation, $e \leq e_{\max} = \lambda_{\min}/4$. Comparison of the FE model results with the exact analytical representation of the sound field in cuboidal rigid cavities [39] showed that this particular e_{\max} value represents a satisfactory trade-off between computational efficiency and low approximation error. The speed of sound and air density are systematically fixed to $c_0 = 343 \text{ m}\cdot\text{s}^{-1}$ and $\rho_0 = 1.21 \text{ kg}\cdot\text{m}^{-3}$, respectively, corresponding to a 20°C room temperature and 50% relative humidity [11]. Fig.4 shows two examples of meshes generated in Ansys, one for a cuboidal reverberation room and the other for a 3-D numerical representation of the KU Leuven reverberation room (abbreviated from here on as KULRR).

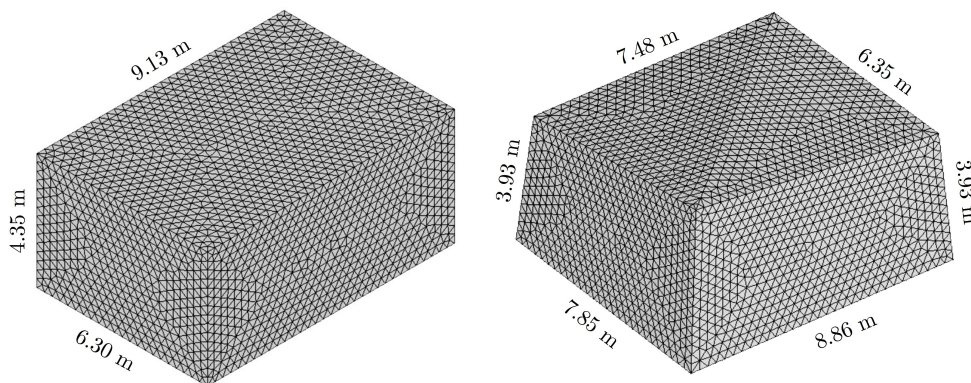


Figure 4: Cuboidal room (left) and KULRR (right) meshed with tetrahedral elements. Some edge lengths corresponding to a scaling to $V_e = 250 \text{ m}^3$ are indicated.

The FE model is validated for cuboidal rooms by quantitatively comparing FRFs resulting from an

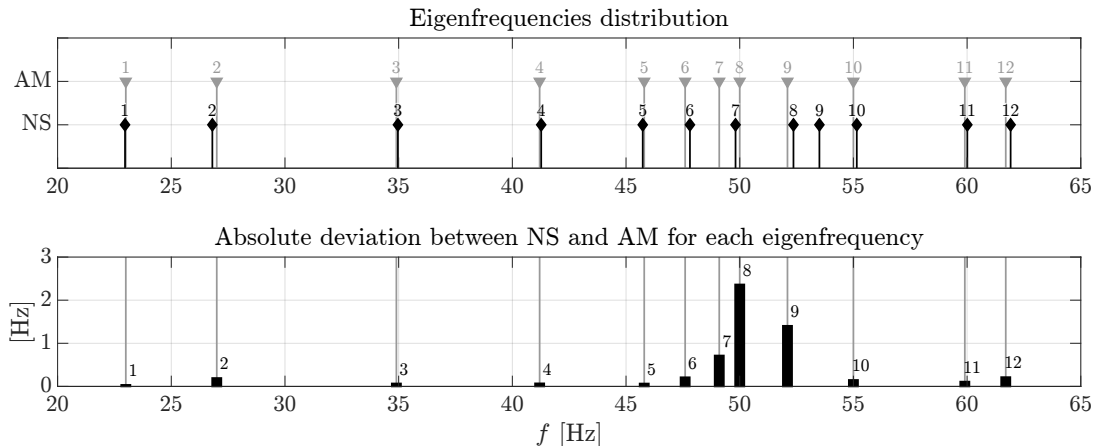


Figure 5: Comparison of KULRR eigenfrequencies between archive measurements (AM) and FE model simulation (NS). The absolute deviation between AM and NS for each eigenfrequency is shown in the lower graph as black bars. Since the archive study does not include information about the mode shapes, the mode numbers are simply assigned based on the increasing value of eigenfrequencies: the lowest eigenfrequency corresponds to mode 1, the second lowest to mode 2, and so on.

undamped FE modal analysis combined with Eq.(6) with FRFs analytically obtained via the closed-form expression of the Green's function in cuboidal rooms [39]. For $f \leq f_{\max} = c_0/(4e_{\max})$, very good agreement is found. For non-regular room geometries, closed-form analytical expressions are unavailable. Instead, a partial low-frequency validation is achieved by conducting a damped modal analysis of an FE model representing the KULRR (right-hand mesh in Fig.4). The model is constructed based on available blueprints and dimensions measured in the actual KULRR. The resulting eigenfrequencies are compared to measured eigenfrequencies from an archive study between 20 and 65 Hz. Within that range, the natural frequencies from the archive study were derived from the clearly separated peaks in measured frequency response functions. Above that frequency the large modal overlap inhibits the confident distinction of room resonances from peaks in the response. The small inherent room damping is included in the FE model using a real-valued impedance boundary condition applied to all surfaces. The value of that impedance is determined for each frequency band via Sabine's equation [9] based on the corresponding values of reverberation times measured in the empty room. Fig.5 shows that a good agreement is generally obtained. The discrepancies found around 50 Hz, as indicated by the black bars in the lower plot, may arise from modelling errors including minor geometric simplifications and from potential uncertainties in the archive measurements themselves.

2.3. Absorptive material model

Once the acoustic domain in the reverberation room is represented numerically, the missing ingredient for using the power balance method described in Section 2.1 is an absorptive material model. In this study, the focus is directed towards porous absorbers and the sample is represented as a locally reacting Delany-Bazley-Miki equivalent fluid [36, 37] whose absorptive characteristics are entirely described by its normalised surface admittance β , itself dependent on the sample's thickness d_s and flow resistivity σ . The local reaction assumption necessary to obtain Eq.(4) generally holds well for porous absorbers with a high flow resistivity or a large thickness [36]. According to Miki [37], this absorber model is valid for frequencies $f/\sigma < 1$. Below 300 Hz, this criterion is fulfilled for a flow resistivity above 300 Nsm^{-4} , which is the case for most realistic porous absorptive materials [40].

The finite nature of the sample, which can lead to observed absorption coefficient values greater than one at low frequencies due to the size effect [1], is represented via the finite surface integral in Eq.(4). In this study, only cuboidal samples are considered. The proposed standard revision ISO/CD 354:2019 [6] recommends an absorptive material covering an area between 10 and 12 m^2 with a length to width ratio between 0.7 and 0.9. Two reference samples respecting these bounds are defined. Sample #1 is a relatively

lightly absorptive material at low frequencies while sample #2 is a highly absorptive material in that range. The latter corresponds to the reference absorber suggested in the ISO/CD 354:2019 [6].

- Sample #1 – $3.0 \times 3.6 \times 0.05 \text{ m}^3$; $\sigma_1 = 30 \text{ kNsm}^{-4}$,
- Sample #2 – $3.0 \times 3.6 \times 0.20 \text{ m}^3$; $\sigma_2 = 10.9 \text{ kNsm}^{-4}$.

2.4. Experimental validation

A validation of the proposed power balance method is performed against experimental data. Recent sound absorption measurements conducted at the Technical University of Denmark (DTU) following the ISO 354:2003 procedure [5, 41] are reproduced by numerical simulation. The DTU 904 reverberation room is modelled and its inherent damping loss factor η_r [cf. Eq.(5)] is adjusted to match the measured reverberation times in the empty reverberation room, as given in [41]. The recorded temperature and relative humidity, as reported in [41], are accounted for by setting the speed of sound accordingly. The source and receiver positions are replicated to the best achievable precision. Fig.6 shows that simulated reverberation time values in the presence of the $2.83 \times 3.48 \times 0.195 \text{ m}^3$ sample of ROCKWOOL FlexiBatt37 [42] used in the measurements (Delany-Bazley-Miki equivalent fluid with $\sigma \approx 13 \text{ kNsm}^{-4}$) agree well with the values measured with two different types of source (omnidirectional and custom-made corner loudspeaker [41]) in the 1/3-octave bands centred between 100 and 250 Hz. These results validate the use of the power balance method as a tool to numerically simulate sound absorption measurements at low frequencies.

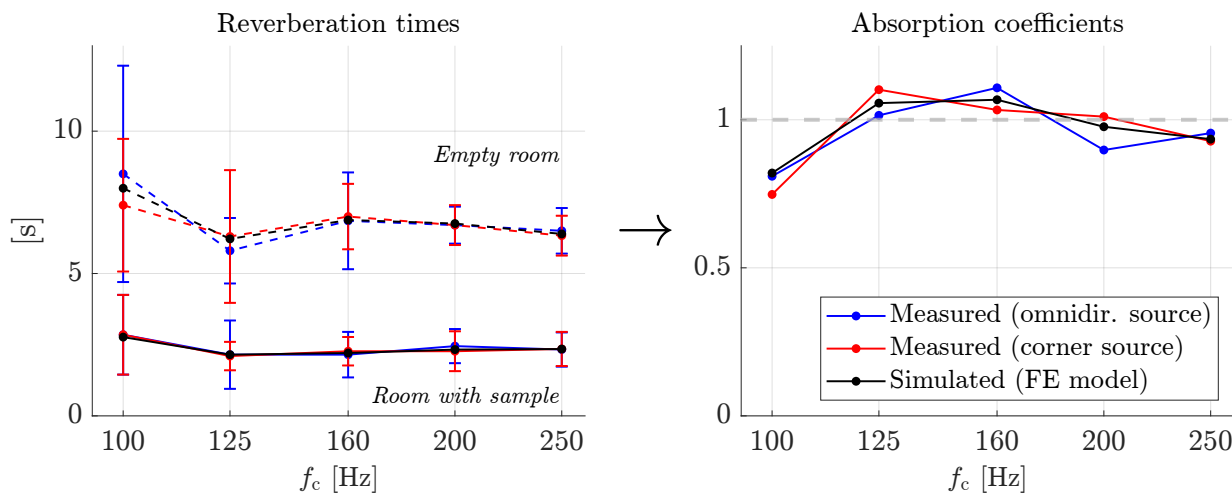


Figure 6: Reverberation times in the DTU reverberation room “904” with and without the presence of a $2.83 \times 3.48 \times 0.195 \text{ m}^3$ sample of ROCKWOOL FlexiBatt37 [42] (left) and corresponding absorption coefficients (right). Simulated values vs. measured values with two different source types from [41]. The error bars represent the spread of reverberation time estimates obtained across the 6 receiver positions used in the measurements.

2.5. Diffuse sound absorption modelling

In order to assess the ability of sound absorption measurements in certain conditions (a given reverberation room, given source and receiver positions, etc.) to yield meaningful results, one must define the values that should be obtained in the most ideal conditions, i.e., in a perfectly diffuse sound field. Although the sound field in a single reverberation room at low frequencies cannot be considered diffuse, as it is heavily influenced by the room modal behaviour, the theoretical diffuse sound absorption emerges as the average result obtained over a large ensemble of reverberation rooms, independently of the room volume, shape, and empty room reverberation time [14]. It has also been demonstrated in [14] that the theoretical diffuse absorption value of a finite-sized sample can be rigorously obtained by application of the diffuse field

reciprocity relationship [15], effectively resulting in a hybrid deterministic-statistical energy analysis (det-SEA) absorber-room model. This approach is also applied here to accurately estimate the theoretical diffuse absorption coefficient of a finite sample of porous absorber that would be measured in ideal diffuse conditions. In the following sections, these diffuse absorption coefficients are used as a benchmark values against which the respective performances of different measurement conditions are evaluated. These benchmark values are systematically denoted α_{diff} from here on. The reader is referred to [14] for more details on the computation of the diffuse reference values.

3. Results across room designs

The reproducibility of sound absorption measurements across different laboratories at low frequencies is assessed using the methodology presented in the previous sections. Sound absorption measurements of the same absorptive materials are simulated across various reverberation room designs in the 1/3-octave bands centred between 100 and 250 Hz. In each room, N_s source positions $\{\mathbf{r}_{0,i}\}_{i=1}^{N_s}$ are defined. For each source position and each 1/3-octave band considered, one sound absorption measurement is simulated and one absorption coefficient α_{sim} is obtained, after integration of the harmonic coefficient via Eq.(3). All sound sources are approximated as point sources of constant unit volume velocity and two different sets of sound source locations are defined. On one hand, eight monopole sources are scattered across the available space, each of them respecting minimum distances to walls, sample, and each other as outlaid in the latest proposed standard revision ISO/CD 354:2019 [6] for microphone positioning. On the other hand, eight monopole sources are placed at eight different corners of the reverberation room. The source is located exactly at the corner position, which corresponds to a real, finite-sized loudspeaker with acoustic centre at that same location. The sample is simulated as laying on the floor of the reverberation room, close to the floor centroid, and rotated by 10° away from the walls meeting at the corner of each reverberation room closest to a right-angled corner. This placement strategy also follows ISO/CD 354:2019 guidelines [6].

Six different reverberation room designs are considered in this part of the study. They are displayed in Fig.7, where the positions used in each reverberation room for the “corner sources” layout are highlighted. The designs are displayed such that the (near-)right-angled corner used as reference for sample rotation is the furthest from the reader. This selection includes three existing designs used in practice [26, 43, 44] (“RR1-2-3”), as well as a perfect cube (“Cube”), a 1:1.45:2.13¹ cuboidal room (“Cuboid”), and the reverberation room design suggested in an annex section of the proposed standard revision ISO/CD 354:2019 [6] (“ISORR”). The last three are theoretical designs that may not correspond to any existing laboratory. As mentioned previously, all reverberation rooms are scaled to 250 m³, a value within the recommended range from the ISO/CD 354:2019 [6]. The inherent damping loss factor η_r of each reverberation room is adjusted via Eq.(1) to obtain an empty-state reverberation time of 10 seconds in all frequency bands. This value was chosen based on the range of reverberation times measured in the empty KULRR in the lowest frequency bands.

In Fig.8, the top row of figures corresponds to the cases where eight sources are placed near corners of the reverberation room, while the bottom row corresponds to the cases involving eight scattered sources. In each row, the results are shown from two perspectives. On the left-hand graphs, averages over values obtained at each source position, $\mathcal{E}_{\mathbf{r}_0}\{\alpha_{\text{sim}}\}$, are shown (where $\mathcal{E}\{\cdot\}$ denotes the expected value operator). On the right-hand graphs, distributions across source positions of the frequency-averaged distance between the absorption coefficients and the diffuse reference values, $\mathcal{E}_{f_c}\{\Delta\alpha\}$, are shown. The core difference between these two measures is the variable over which the average is performed, namely source positions for the former against 1/3-octave bands for the latter. The measures are explicitly defined in Eqs. (10) and (11), respectively, where the i^{th} centre-band frequency is denoted $f_{c,i}$ and N_b refers to the number of 1/3-octave bands considered.

¹The cuboidal room dimension ratios are defined here as $r_{xy} = L_x/L_y$ and $r_{xz} = L_x/L_z$, where L_x , L_y , and L_z are the length, width, and height of the room, respectively. To refer to a room with specific dimension ratios, the notation 1: r_{xy} : r_{xz} is adopted.

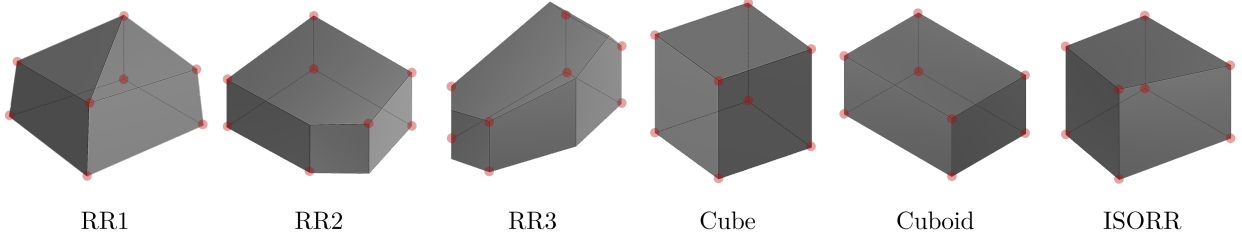


Figure 7: Reverberation room designs tested. Labels used in this study are indicated below each design. The red dots indicate the eight positions used for the “corner sources” configuration in each room. No added diffusers are present in the rooms.

$$\mathcal{E}_{\mathbf{r}_0}\{\alpha_{\text{sim}}\}(f_c) = \frac{1}{N_s} \sum_{i=1}^{N_s} \alpha_{\text{sim}}(f_c, \mathbf{r}_{0,i}), \quad (10)$$

$$\mathcal{E}_{f_c}\{\Delta\alpha\}(\mathbf{r}_0) = \frac{1}{N_b} \sum_{i=1}^{N_b} |\alpha_{\text{sim}}(f_{c,i}, \mathbf{r}_0) - \alpha_{\text{diff}}(f_{c,i})|. \quad (11)$$

The results obtained in the presence of the lightly absorptive sample (#1) suggest that most reverberation rooms considered perform equivalently well for low absorption coefficients. These results show that a highly absorptive sample should be preferred to a lightly absorptive sample as reference material when evaluating reverberation room designs, as potent absorbers naturally exacerbate the differences between α_{sim} values obtained in each reverberation room. This finding goes in the direction suggested in the proposed standard revision ISO/CD 354:2019 [6], which recommends the use of a reference absorber with an absorption coefficient close to unity across the entire frequency range.

The strongest disparities across reverberation room designs are obtained in the presence of sample #2, for both source arrangements. It can be noted that, as expected, the theoretical diffuse value matches the average absorption across all reverberation rooms well. Nevertheless, there is a clear difference between the results for the individual rooms with corner sources and with scattered sources. When scattered sources are employed, the position-averaged absorption coefficient $\mathcal{E}_{\mathbf{r}_0}\{\alpha_{\text{sim}}\}$ of a single room tends to result in both positive and negative deviations from the diffuse reference value, depending on the frequency band. However, for the corner sources, $\mathcal{E}_{\mathbf{r}_0}\{\alpha_{\text{sim}}\}$ tends to result in more systematic differences. This is clearly visible for the cubic reverberation room, where the position-averaged absorption coefficient $\mathcal{E}_{\mathbf{r}_0}\{\alpha_{\text{sim}}\}$ for corner sources is larger than the reference value in all 1/3-octave bands centred above 100 Hz. It has been confirmed by additional simulations (not reproduced here) that this systematic difference depends on the room volume and the sample placement; for example, the systematic overestimation of the absorption coefficient changes into a systematic underestimation when the room volume is reduced to 200 m³. Similar systematic differences are observed for the non-symmetric rooms RR1 and RR3. Furthermore, the scatter of $\mathcal{E}_{\mathbf{r}_0}\{\alpha_{\text{sim}}\}$ across the different rooms is larger for the corner sources than for the scattered sources.

These results indicate that different corner positions in the same room tend to have a similar effect on the obtained absorption value and therefore averaging across such positions has a limited effect on the reproducibility. This is confirmed by the other plots in Fig.8, which display the frequency-averaged absolute deviations from the reference value, $\mathcal{E}_{f_c}\{\Delta\alpha\}$, for each room. For most rooms, the scatter of these values across the different source positions is significantly lower for the corner sources than for the scattered sources. When corner sources are used, the results are indeed found not to vary drastically when using more than two sources, which is the minimum number recommended in the ISO 354:2003 [5]. The extreme case is offered by the cubic room where, due to the symmetry, different corner source positions tend to result in very similar absorption values. Whether these values are close to the diffuse reference values depends, amongst other things, on the room geometry. Interestingly, the cuboidal room yields the best performance across the investigated reverberation rooms with sample #2 using corner sources. This relates to the fact that,

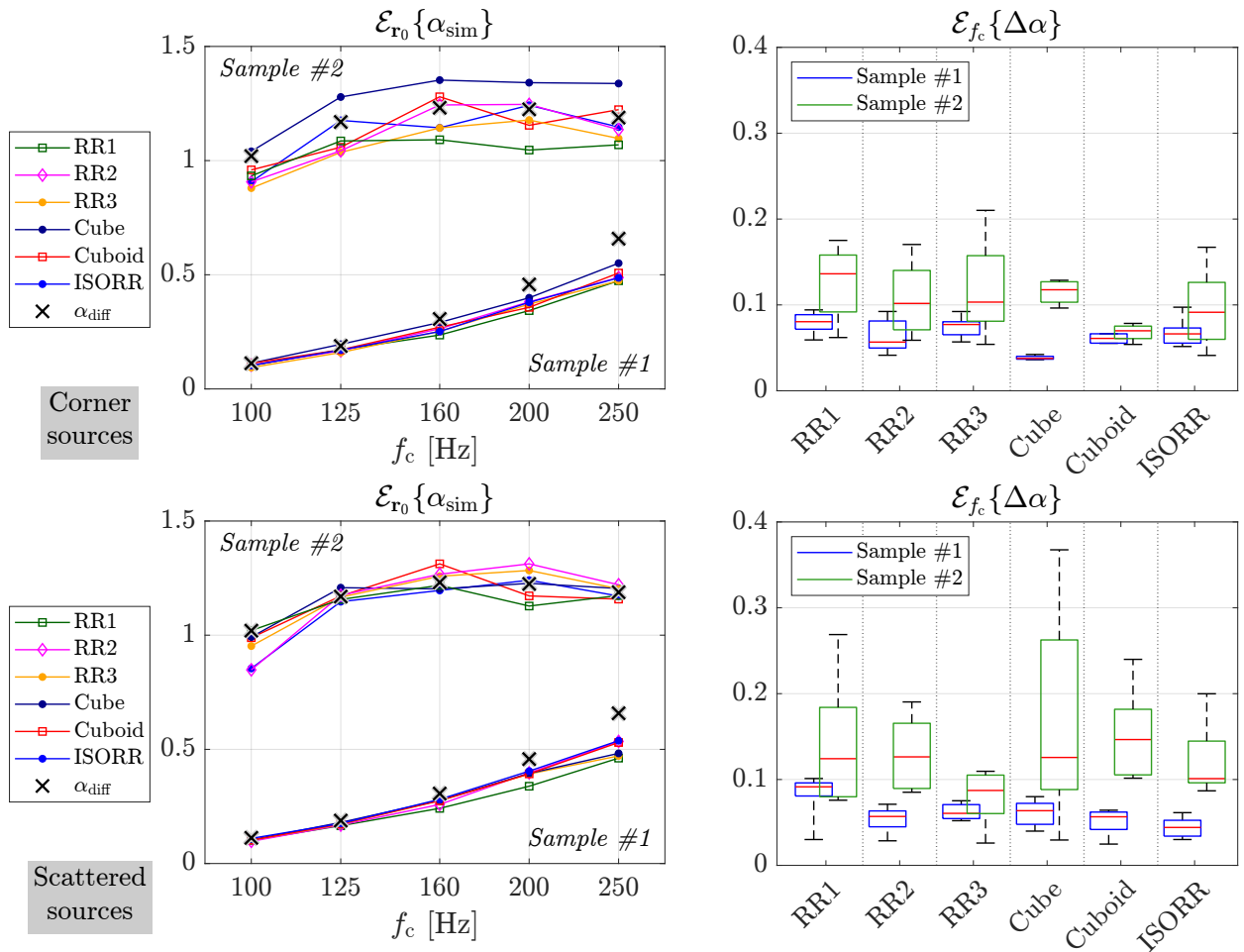


Figure 8: Absorption coefficients across reverberation room designs for sample #1 ($3.0 \times 3.6 \times 0.05 \text{ m}^3$, $\sigma_1 = 30 \text{ kNsm}^{-4}$) and sample #2 ($3.0 \times 3.6 \times 0.2 \text{ m}^3$, $\sigma_2 = 10.9 \text{ kNsm}^{-4}$). Simulations conducted for eight individual sources exactly at room corners (upper graphs) or scattered across the available volume (lower graphs). Left: averages over results obtained at each source position as function of frequency [Eq.(10)]. Right: distributions of frequency-averaged distances between simulated absorption coefficients and diffuse reference values across source positions [Eq.(11)]. The red segments mark the median distances across sources, the top and bottom box edges the 25th and 75th percentiles, and the whiskers reach the most extreme data points.

for a 250 m^3 volume, the particular dimension ratios 1:1.45:2.13 ensure a homogenous spread of natural frequencies of the hard-walled reverberation room along the frequency axis.

While the results reported in Fig.8 indicate that averaging across scattered source positions could be a strategy for obtaining absorption coefficients that are close to the diffuse reference values, it is also clear from the same figure that the variability across these source positions strongly depends on the room geometry. This is further investigated in Fig.9, where the analysis is repeated 50 times to yield 50 different sets of scattered source positions for the cubic room and for RR3. In RR3, fewer source positions are required to achieve the same accuracy. The cubic room is again an extreme case where different scattered source positions lead to very different values because the symmetry results in a highly uneven distribution of natural frequencies across the frequency axis. Finally, from Fig.8, it is observed that RR3 performs clearly better when using source positions scattered across the room volume than when using corner sources. It is therefore important to consider the source positioning and the room geometry together.

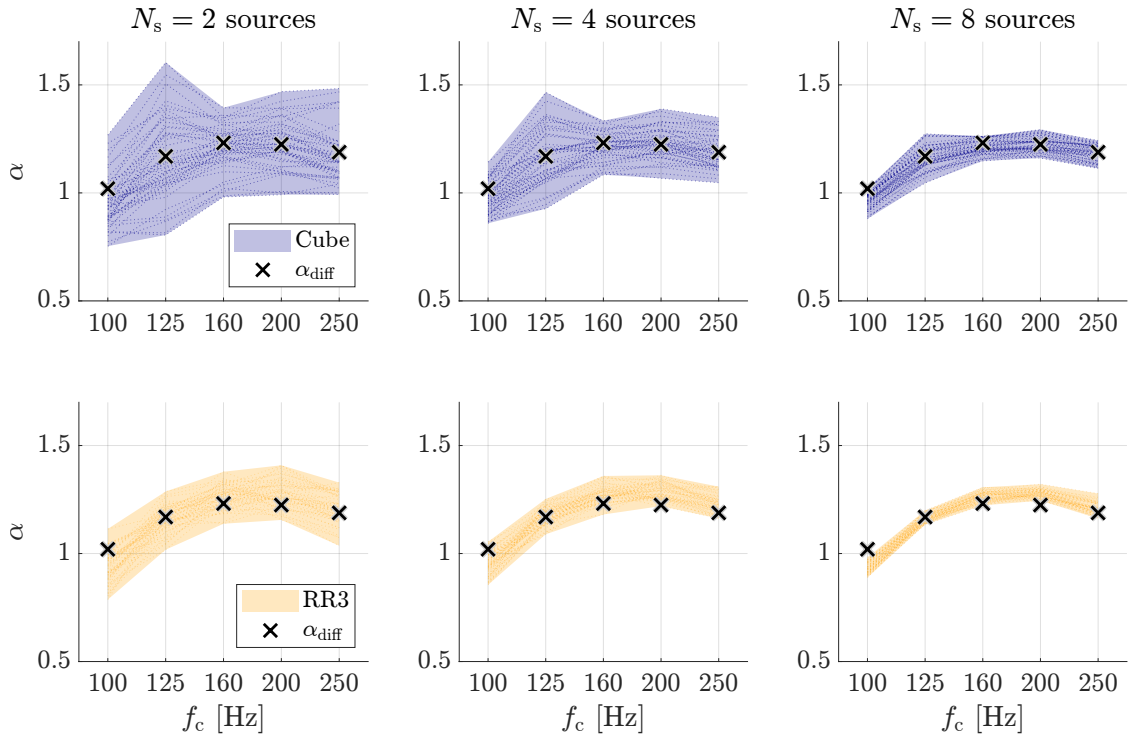


Figure 9: Distributions of simulated absorption coefficients obtained in the cubic reverberation room (upper graphs) or in RR3 (lower graph) across 50 different sets of N_s scattered source positions. N_s takes the value 2 (left), 4 (middle), or 8 (right).

4. Diffusing elements

In this section, curved panel diffusers are introduced in the FE model. Their effect on sound absorption measurements has been experimentally investigated in the past [7, 8, 45], directing the focus towards mid-to high-frequency. This section provides an assessment of the effect of curved panel diffusers on sound absorption measurements below 300 Hz, comparing the simulated absorption coefficients to their theoretical diffuse counterparts.

The panel diffusers are modelled as $1 \times 1.5 \text{ m}^2$ curved rectangular sheets with a 1 metre curvature radius and a 5 centimetres thickness. These dimensions are within the bounds given in the latest proposed standard revision ISO/CD 354:2019 [6]. The considered panels are relatively thick because they approximate thin bent plastic panels supported by individual wooden frames. The panels are introduced directly inside the FE model as rigid volumes. For every number of panels and every panels arrangement, a new FE mesh is generated. Through two constraints, all simulated panel arrangements respect the corresponding ISO/CD 354:2019 [6] guidelines: (i) A minimum distance of one curvature radius between the back of the panel and the closest reverberation room surfaces is systematically ensured to avoid sound-shadowing zones; (ii) Each panel is oriented such that its convex side faces the sample. Sound absorption measurements of sample #1 and #2 (cf. Section 2.3) are simulated in the reverberation room design suggested in the Annex of ISO/CD 354:2019 [6] and in a 1:1:1.22 cuboidal reverberation room, varying the number N_p of panel diffusers present. The 1:1:1.22 cuboid was chosen as a contrasting option with respect to the relatively well-performing ISORR (see Section 3). It was indeed found to yield a particularly poor correspondence between measured and theoretical absorption coefficients (in the absence of diffusers) in the low-frequency range, while remaining a valid geometry within the bounds imposed on room longest diagonal length and floor surface area formulated in the ISO/CD 354:2019 [6]. For each number of diffusers ($N_p \in \{0, 2, 4, 6, 8, 10, 15\}$), six different panel arrangements are generated. Sound absorption measurement simulations are conducted with each of these arrangements, following the methodology described in Section 2, and the results are averaged to maintain

420 the focus on the variable of interest: N_p .

Each panel diffusers arrangement is generated incrementally, introducing one panel at a time in the reverberation room. A random point is selected in the available volume, corresponding to the panel's centre of mass. The panel orientation is then determined in two steps. First, the azimuthal angle between the panel's local Cartesian coordinate system and the global coordinate system is chosen randomly. Second, the polar angle is chosen to ensure that the convex side of the panel faces the sample. If the newly introduced panel is sufficiently distant from walls and other panels, it is kept. Otherwise, the panel is discarded and a new one is generated at another position with another orientation. The incremental panel addition procedure is repeated until the desired number of panels is attained. Two examples of panel arrangements are shown in Fig.10.

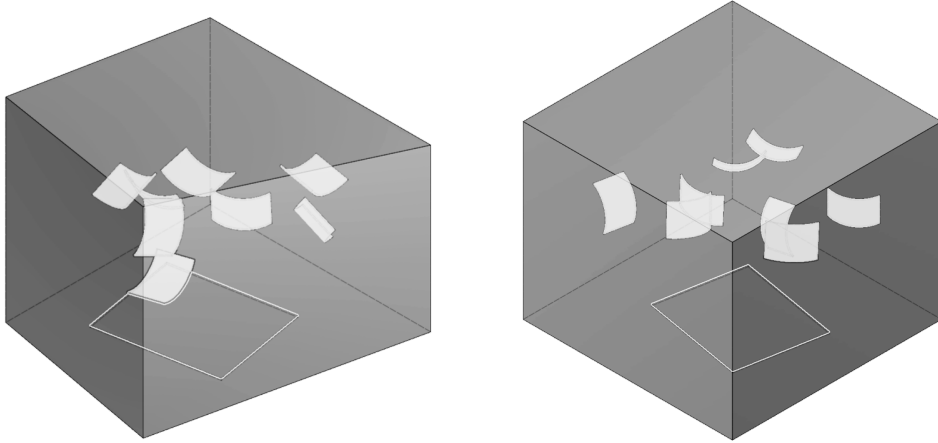


Figure 10: Examples of $N_p = 8$ panels arrangements in ISORR (left) and the 1:1:1.22 cuboidal reverberation room (right).

430 The use of randomly generated panel diffuser locations and orientations inhibits the use of a unique set of scattered source positions across panel arrangements, as the minimum 1-metre panel-source distance may not be respected in certain cases. Therefore, only corner source positions are used in this part of the study. In both reverberation rooms, the eight available corner source positions are used. The solutions are computed in the presence of all eight decorrelated monopole sources simultaneously, following Eq.(9).
435 in the preceding reproducibility study, the sample is placed close to the floor centroid to ensure a minimum distance of 1 metre to the walls. It is rotated by 10° from the right-angled corner of the reverberation room, following the recommendation formulated in the proposed standard revision ISO/CD 354:2019 [6]. Here again, the inherent reverberation room damping loss factor η_r is adjusted to obtain an empty-room reverberation time T_e of 10 seconds via Eq.(1). The reduction in the effective volume of air caused by the
440 presence of diffusers is accounted for when computing α_{sim} via Eq.(2): V_e is replaced by $V_e - V_{diff}$ and V_s is replaced by $V_s - V_{diff}$, where V_{diff} is the combined volume of all panel diffusers.

Similarly to what was observed in the reproducibility study discussed in Section 3, the results obtained in the presence of a lightly absorptive sample (#1) provide only limited information, as the results vary insignificantly from one number of panel diffusers to another. The focus of the following discussion will thus
445 be directed towards the highly absorptive sample (#2).

When simulating the measurement of sample #2 in the 1:1:1.22 cuboid, the panels seem to improve the agreement between α_{sim} and α_{diff} over the frequency bands considered. Indeed, with an increasing number of panels, the absorption coefficients converge towards the diffuse reference values in all 1/3-octave bands, which is the expected outcome of an increase in sound field diffusivity. These results show that large
450 diffusing elements may be beneficial for low-frequency sound absorption measurements of highly absorptive materials in unideal reverberation room geometries. This observation agrees well with the conclusions of another numerical study of the effect of panel diffusers conducted by Toyoda et al. [7]. Conversely, the

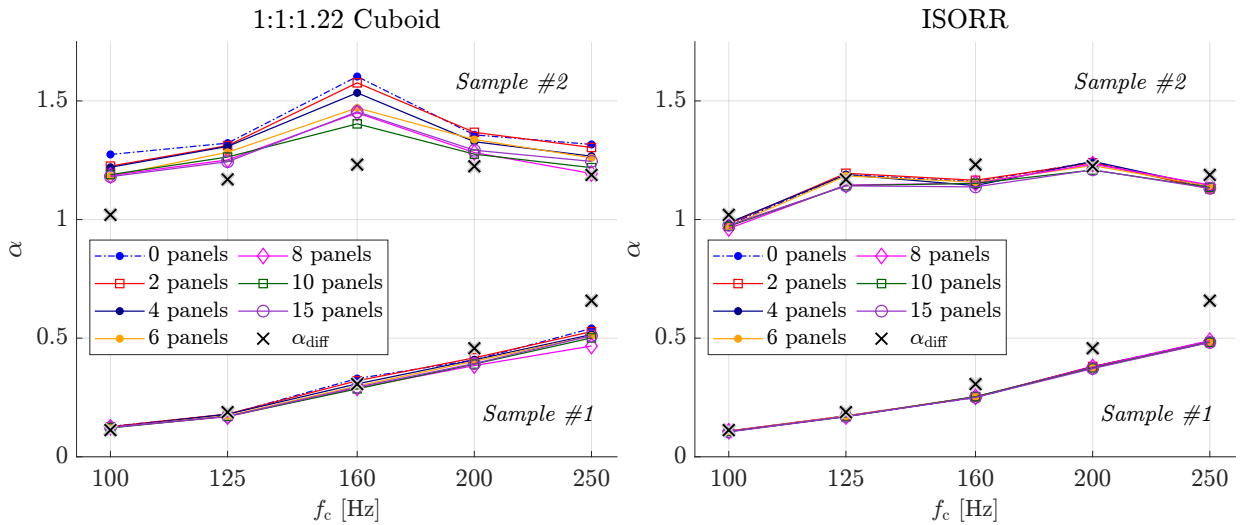


Figure 11: Absorption coefficients of sample #1 (lower sets of lines) and #2 (upper sets) simulated in ISORR (left plot) or in a 1:1:1.22 cuboidal reverberation room (right plot), varying the number of panel diffusers. Each value is an average over six randomly generated panel arrangements and eight corner source positions.

effect of panel diffusers appears to be insignificant in ISORR for both samples, as α_{sim} remains consistently close to α_{diff} in all bands considered. These results suggest that room geometry not only has an impact on the sound absorption coefficients resulting from measurements, but also on the potential usefulness of panel diffusers at low frequencies. These results agree with those obtained in a recent study [46], where the impact of panel diffusers on the spatial standard deviation of sound pressure level at low frequencies in a reverberation room with nonparallel walls (similar to ISORR) was investigated via numerical simulations results combined with experimental data.

Interestingly, results simulated in the cuboidal reverberation room seem to stabilise above a certain number of panels, reaching a stable sound field state. Namely, going from 10 to 15 panel diffusers does not provide any significant change in results when measuring sample #2, although the results still overestimate α_{diff} in the lowest frequency bands, unlike those obtained in ISORR. This observation can be related to the ISO 354:2003 [5] recommendations on room diffusivity, advising the iterative introduction of diffusers until measurement results converge. The ISO 354:2003 [5] standard states that, in cuboidal rooms, the double-sided area of diffusers required to achieve satisfactory diffusion falls roughly between 15% and 25% of the total room surface area. These bounds are justified by the typical range of values found experimentally [47]. The 250 m³ 1:1:1.22 cuboid has a total surface area of 209 m² and the panel diffusers have an individual double-sided surface area of 3 m². The indicative 15-25% bounds here suggests that optimal diffusivity can be expected to be reached when introducing between 11 and 17 diffusers. This relates well to Fig.11, where using 8 or more panels leads to very similar performances. It may also be noted that introducing 15 panels (double-sided diffusers area is then 21% of the room surface area) yields a slightly poorer performance in the 160 Hz- and 250 Hz-centred bands than with only 10 panels. This indicates that a too large number of panels may somewhat hinder the reverberation room's performance. Davy et al. [48] also underlined that the type of spatial arrangement chosen for the diffusers may also be able to influence this "optimal" number of panels. In the latter study, panels were not distributed throughout the room (as in Fig.10) but instead located in a restricted zone near walls. In those conditions, the minimum number of panels needed to reach consistent measured sound absorption values was found visibly higher than in the previously mentioned study by Benedetto et al. [47]. The specific type of panel arrangement to be adopted is therefore another important aspect to consider when formulating recommendations on the use of panel diffusers.

It appears advisable to decide on a sufficient yet reasonably limited number of diffusers in this case, e.g., by following the methodology outlined in Annex A of the ISO 354:2003 standard [5]. The simulated results suggest that reaching a stable result via the iterative introduction of panel diffusers does not neces-

sarily imply achieving a perfect agreement between measured and theoretical diffuse absorption coefficients at low frequencies. Increasing the size of the panel diffusers may also be expected to further benefit the correspondence between measured and theoretical absorption coefficients in rooms with many parallel surfaces. Other factors such as the reverberation room geometry itself may also remain dominant, as was underlined in Section 3. One should keep in mind that the introduction of diffusing elements, although helpful, cannot be expected to fully account for poor reverberation room design.

5. Conclusions

A computationally efficient methodology for the simulation of sound absorption measurements at low frequencies, using a FE model combined with a power balance method, was presented and validated against more detailed simulations and experimental data. The model was subsequently employed for assessing the differences between sound absorption values measured in a specific room and the diffuse reference values, which emerge as the ensemble average values across a wide range of rooms, also at low frequencies. The results confirmed the lack of reproducibility observed in the outcomes of round robin studies, as well as the often clear deviations from the diffuse reference absorption coefficients. The choice of main room dimension ratios appeared as a potentially crucial aspect of reverberation room design for minimising those deviations in the low end of the spectrum, more so than the presence of only nonparallel surfaces. Two source positioning strategies were investigated: corner positions and scattered positions. Corner positions typically yield better repeatability, but averaging over them does not always lead to better diffusivity and therefore not to better reproducibility. In contrast, averaging over many scattered source positions can consistently lead to better diffusivity in a variety of room geometries, as long as a sufficiently large number of positions is used. In fact, too few scattered sources may negatively impact repeatability and reproducibility in certain room designs. The results conclusively show that room geometry and source positioning strategy should be considered jointly when addressing sound absorption measurement reproducibility. Additionally, some results suggested that panel diffusers may have a beneficial impact on the results at low frequencies in certain conditions, namely when measuring a potent absorptive material in a reverberation room with many parallel walls.

Since the number of considered simulation conditions is relatively limited for practical reasons, the applicability of the conclusions drawn is restricted to measurements conducted in similar conditions, namely in a reverberation room close to 250 m³, with a rectangular, centred, and highly absorptive sample on its floor. The same simulation methodology may nevertheless be used to compute and inspect a more exhaustive simulation results set, covering a wide range of reverberation room designs. As the parameters investigated in this study were found to have clear impacts on the outcomes of sound absorption measurements at low frequencies, the investigation may also be valuably extended towards other measurement aspects that could not be included in the present study. Namely, assessing the impact of inherent room damping, sample placement and orientation, number and placement of receiver, or sample size through the simulation framework presented in this work would provide further beneficial insights when aiming at identifying conditions that best favour the reproducibility and accuracy of sound absorption measurements. Furthermore, although the context of this study was set below 300 Hz, which is the most critical frequency range in terms of poor measurement reproducibility, it would be possible to explore different frequency ranges following the same methodology. Other potential extensions of this work may include, for example, the use of different absorptive materials and other types of diffusing elements.

Acknowledgments

The authors would like to thank ROCKWOOL A/S International for funding this research; Rasmus Gottrup Barfod and Mads Bolberg from ROCKWOOL A/S International for helpful discussions; Gerrit Vermeir from KU Leuven for providing data for the KU Leuven reverberation room; and Cheol-Ho Jeong and Niels P. Moos from DTU for detailed information on the DTU validation data.

530 **References**

- [1] C.W. Kosten. International comparison measurements in the reverberation room. *Acustica*, 10(5–6):400–411, 1960.
- [2] Y. Makita. Investigations into the precision of measurement of sound absorption coefficients in a reverberation room (I)–The 3rd round robin test and the investigations on the diffusivity of sound field. *Journal of the Acoustical Society of Japan*, 24:381–392, 1968.
- 535 [3] M.R. Schroeder and R. Gerlach. Diffusion, room shape and absorber location – influence on reverberation time. *Journal of the Acoustical Society of America*, 56(4):1300, 1974.
- [4] C. Scrosati, F. Maretlotta, F. Pompoli, A. Schiavi, A. Prato, D. D’Orazio, M. Garai, N. Granzotto, A. Di Bella, F. Scamoni, M. Depalma, C. Marescotti, F. Serpilli, V. Lori, P. Nataletti, D. Annesi, A. Moschetto, R. Baruffa, G. De Napoli, F. D’Angelo, and S. Di Filippo. Towards more reliable measurements of sound absorption coefficient in reverberation rooms: an inter-laboratory test. *Applied Acoustics*, 165(107298):1–19, 2020.
- 540 [5] International Organization for Standardization. *ISO 354: Acoustics – Measurement of sound absorption in a reverberation room*, 2003.
- [6] International Organization for Standardization. *Circulation of the Committee Draft ISO/CD 354*, 2019.
- [7] E. Toyoda, S. Sakamoto, and H. Tachibana. Effects of room shape and diffusing treatment on the measurement of sound absorption coefficient in a reverberation room. *Acoustical Science and Technology*, 25(4):255–266, 2004.
- 545 [8] M. Nolan, M. Vercammen, and C.-H. Jeong. Effects of different diffuser types on the diffusivity in reverberation chambers. In *Proceedings of Euronoise 2015 Maastricht, The Netherlands, 31 May-3 June*, pages 191–196, 2015.
- [9] P.E. Sabine. The measurement of sound absorption coefficients. *Journal of The Franklin Institute*, 207(3):341–368, 1929.
- [10] M.R. Schroeder. New method of measuring reverberation time. *Journal of the Acoustical Society of America*, 37(3):409–412, 1965.
- 550 [11] F. Jacobsen and P.M. Juhl. *Fundamentals of general linear acoustics*. John Wiley & Sons, Chichester, UK, 2013.
- [12] H. Dekker. Edge effect measurements in a reverberation room. *Journal of Sound and Vibration*, 32(2):199–202, 1974.
- [13] A. Cops, J. Vanhaecht, and K. Leppens. Sound absorption in a reverberation room: Causes of discrepancies on measurement results. *Applied Acoustics*, 46(3):215–232, 1995.
- 555 [14] C. Van hoorickx, P. Didier, and E.P.B. Reynders. Prediction and uncertainty quantification of the diffuse sound absorption of finite absorbers. *Journal of Sound and Vibration*, 539(117258):1–17, 2022.
- [15] P.J. Shorter and R.S. Langley. On the reciprocity relationship between direct field radiation and diffuse reverberant loading. *Journal of the Acoustical Society of America*, 117(1):85–95, 2005.
- [16] P.J. Shorter and R.S. Langley. Vibro-acoustic analysis of complex systems. *Journal of Sound and Vibration*, 288(3):669–699, 2005.
- 560 [17] E.P.B. Reynders and R.S. Langley. Cross-frequency and band-averaged response variance prediction in the hybrid deterministic-statistical energy analysis method. *Journal of Sound and Vibration*, 428:119–146, 2018. Open access.
- [18] E. Reynders, R.S. Langley, A. Dijkmans, and G. Vermeir. A hybrid finite element - statistical energy analysis approach to robust sound transmission modelling. *Journal of Sound and Vibration*, 333(19):4621–4636, 2014.
- 565 [19] J.C.E. Van den Wyngaert, M. Schevenels, and E.P.B. Reynders. Predicting the sound insulation of finite double-leaf walls with a flexible frame. *Applied Acoustics*, 141:93–105, 2018.
- [20] E.P.B. Reynders, P. Wang, C. Van hoorickx, and G. Lombaert. Prediction and uncertainty quantification of structure-borne sound radiation into a diffuse field. *Journal of Sound and Vibration*, 463:114984, 2019.
- [21] P. Wang, C. Van hoorickx, G. Lombaert, and E. Reynders. Numerical prediction and experimental validation of impact sound radiation by timber joist floors. *Applied Acoustics*, 162(107182):1–17, 2020.
- 570 [22] M. Meissner. Prediction of low-frequency sound field in rooms with complex-valued boundary conditions on walls. *Vibrations in Physical Systems*, 30(1):1–8, 2019.
- [23] L. Savioja and U.P. Svensson. Overview of geometrical room acoustic modeling techniques. *Journal of the Acoustical Society of America*, 138(2):708–730, 2015.
- 575 [24] R. Prislán and D. Svenšek. Ray-tracing semiclassical (RTS) low frequency acoustic modeling validated for local and extended reaction boundaries. *Journal of Sound and Vibration*, 437:1–15, 2018.
- [25] G. Benedetto and R. Spagnolo. Evaluation of sound absorbing coefficients in a reverberant room by computer-ray simulation. *Applied Acoustics*, 17(5):365–378, 1984.
- [26] A. Alonso and F. Martellotta. Room acoustic modelling of textile materials hung freely in space: from the reverberation chamber to ancient churches. *Journal of Building Performance Simulation*, 9(5):469–486, 2016.
- 580 [27] C. Scrosati, F. Scamoni, M. Depalma, and N. Granzotto. On the Diffusion of the Sound Field in a Reverberation Room. In *Proceedings of the 26th International Congress on Sound and Vibration, ICSV 2019, Montreal, Canada, 7-11 July*, 2019.
- [28] N.B. Roozen, E.A. Piana, E. Deckers, and C. Scrosati. On the numerical modelling of reverberation rooms, including a comparison with experiments. In *Proceedings of the 26th International Congress on Sound and Vibration, ICSV 2019, Montreal, Canada, 7-11 July*, 2019.
- 585 [29] R. Tomiku, T. Otsuru, and Y. Takahashi. Finite element sound field analysis of diffuseness in reverberation rooms. *Journal of Asian Architecture and building engineering*, 1(2):33–39, 2002.
- [30] R. Tomiku, T. Otsuru, N. Okamoto, and Y. Kurogi. Direct and modal frequency response analysis of sound fields in small rooms by finite element method. *Journal of the Acoustical Society of America*, 123(5):3092, 2008.
- 590 [31] T. Okuzono, N. Shimizu, and K. Sakagami. Predicting absorption characteristics of single-leaf permeable membrane absorbers using finite element method in a time domain. *Applied Acoustics*, 151:172–182, 2019.

- [32] N. Sakamoto, T. Otsuru, R. Tomiku, I. Eto, D. Matsuoka, and R. Yoshimoto. Investigating the practicability of an ensemble averaging method for measuring sound absorption and surface normal impedance. *Applied Acoustics*, 156:166–175, 2019.
- 595 [33] L. Meirovitch. *Elements of vibration analysis*. McGraw-Hill, New York, NY, 1975.
- [34] N. Atalla and F. Sgard. *Finite element and boundary element methods in structural acoustics and vibration*. CRC Press, Boca Raton, FL, 2015.
- [35] M. Nolan, S.A. Verburg, J. Brunskog, and E. Fernandez-Grande. Experimental characterization of the sound field in a reverberation room. *Journal of the Acoustical Society of America*, 145(4):2237–2246, 2019.
- 600 [36] M.A. Delany and E.N. Bazley. Acoustical properties of fibrous materials. *Applied Acoustics*, 3(2):105–116, 1970.
- [37] Y. Miki. Acoustical properties of porous materials - modifications of Delany-Bazley models. *Journal of the Acoustical Society of Japan*, 11(1):19–24, 1990.
- [38] Ansys, Inc. Introduction to Ansys Mechanical APDL. <https://www.ansys.com/training-center/course-catalog/structures/introduction-to-ansys-mechanical-apdl>. [Online; accessed 16-Sept-2021].
- 605 [39] P.M. Morse and K.U. Ingard. *Theoretical Acoustics*. McGraw-Hill, New York, NY, 1968.
- [40] R. Dragonetti, C. Ianniello, and R.A. Romano. Measurement of the resistivity of porous materials with an alternating air-flow method. *Journal of the Acoustical Society of America*, 129(2):753–764, 2011.
- [41] N.P. Moos. Bachelor’s project: Loudspeaker configuration for ISO 354. DTU, January 2021.
- [42] Rockwool A/S. *Flexibatts 37 documentation*. www.rockwool.dk/produkter/bygningsisolering/flexibatts-37/. [Online; accessed 30-Aug-2021].
- 610 [43] H. Myncke. Bouwkundige aspekten van de akoestische meetruimten van de Katholieke Universiteit te Leuven. *Het Ingenieursblad*, 36(21):651–659, 1967.
- [44] Y.H. Bakhtiar, S. Indrawati, and M. Suyatno. Evaluation of reverberation chamber relation to reverberation time and distribution of sound pressure level with ISO 354 as standard in building physics laboratory of physics department ITS. *Journal of Physics: Conference Series*, 1153, 2019.
- 615 [45] D.T. Bradley, M. Müller-Trapet, J. Adelgren, and M. Vorländer. Effect of boundary diffusers in a reverberation chamber: Standardized diffuse field quantifiers. *Journal of the Acoustical Society of America*, 135(4):1898–1906, 2014.
- [46] S. Wang, J. Zhong, X. Qiu, and I. Burnett. A note on using panel diffusers to improve sound field diffusivity in reverberation rooms below 100 Hz. *Applied Acoustics*, 169:107471, 2020.
- 620 [47] G. Benedetto, E. Brosio, and R. Spagnolo. The effect of stationary diffusers in the measurement of sound absorption coefficients in a reverberation room: An experimental study. *Applied Acoustics*, 14(1):49–63, 1981.
- [48] J.L. Davy, W.A. Davern, and P. Dubout. Qualification of room diffusion for absorption measurements. *Applied Acoustics*, 28(3):177–185, 1989.